agronomy

MDPI

*Article*

# TaNSUN2-Mediated m$^5$C Modification of *TaTHI2* Modulates Antiviral Immunity Against Chinese Wheat Mosaic Virus

**Liwen Chen [1,2,3,4,†], Meichen Zhang [1,2,3,4,†], Yulun Wu [1,5], Lixiao Feng [1,2,3,4], Ying Liu [1,2,3,4], Jiaqian Liu [1,2,3,4], Jian Yang [1,2,3,4,*] and Yaoyao Jiang [1,2,3,4,*]**

1 Key Laboratory for Quality and Safety of Agro-Products, Ningbo University, Ningbo 315211, China; chenliwen0621@163.com (L.C.); zhangmeichen0911@163.com (M.Z.); m19973879018@163.com (Y.W.); fenglixiao@hnu.edu.cn (L.F.); ly1410147326@163.com (Y.L.); jiaqianliu2020@163.com (J.L.)
2 Key Laboratory of Biotechnology in Plant Protection, Ministry of Agriculture and Rural Affairs, Ningbo University, Ningbo 315211, China
3 Key Laboratory of Green Plant Protection of Zhejiang Province, Ningbo University, Ningbo 315211, China
4 Institute of Plant Virology, Ningbo University, Ningbo 315211, China
5 Institute of Plant Protection, Longping College of Agronomy, Hunan University, Changsha 410082, China
* Correspondence: nather2008@163.com (J.Y.); yyaojiang@163.com (Y.J.)
† These authors contributed equally to this work.

## Abstract

Although RNA cytosine-5 methylation (m$^5$C) is an important post-transcriptional regulatory mechanism, its contribution to plant antiviral immunity remains unclear. In this study, we identified Thiamine thiazole synthase 2 (TaTHI2) as a host mRNA target of the wheat m$^5$C methyltransferase TaNSUN2 during infection by Chinese wheat mosaic virus (CWMV), a soil-borne virus that poses a major threat to wheat production. TaNSUN2 contributes to the m$^5$C modification of *TaTHI2* transcripts, enhancing mRNA stability and sustaining *TaTHI2* accumulation. The disruption of a key m$^5$C site markedly reduced methylation, weakened TaNSUN2–RNA binding, and accelerated transcript decay, leading to the compromised production of reactive oxygen species (ROS) and increased viral infection. Mechanistically, the TaNSUN2-dependent m$^5$C modification stabilized *TaTHI2* mRNA, thereby promoting ROS-mediated antiviral defense. Collectively, our results establish the m$^5$C modification of *TaTHI2* mRNA as a critical post-transcriptional control point in CWMV resistance and highlight TaNSUN2-dependent RNA methylation as an integral component of host antiviral immunity.

**Keywords:** RNA m$^5$C methylation; TaNSUN2; TaTHI2; antiviral immunity; Chinese wheat mosaic virus

Check for updates

Academic Editor: Khalid Amari

Received: 30 March 2026
Revised: 26 April 2026
Accepted: 29 April 2026
Published: 30 April 2026

**Copyright:** © 2026 by the authors. Licensee MDPI, Basel, Switzerland. This article is an open access article distributed under the terms and conditions of the Creative Commons Attribution (CC BY) license.

## 1. Introduction

Post-transcriptional RNA modifications constitute a pervasive regulatory layer that shapes gene expression across living organisms [1–3]. To date, more than 170 chemically distinct RNA modifications have been identified, primarily in mRNA, tRNA, and rRNA [4–6]. Among these, several mRNA modifications, including N6-methyladenosine (m$^6$A), N1-methyladenosine (m$^1$A), 5-methylcytosine (m$^5$C), and N7-methylguanosine (m$^7$G), have emerged as important modulators of RNA fates [4,7]. RNA modifications have also emerged as novel and efficient targets in responses against viruses [8], and accumulating evidence suggests that they further participate in plant stress responses and immune regulation, fine-tuning transcript stability, translation efficiency, and signaling outputs during pathogen challenge. In particular, both m$^6$A and m$^5$C modifications have been implicated

in plant–pathogen challenges, highlighting RNA modifications as integral components of post-transcriptional immune control [9–12].

Among these modifications, $m^5C$ is a conserved yet comparatively understudied mRNA alteration [13]. Members of the NOP/Sun (NSUN) family—which includes NSUN2 in mammals and TRM4B in *Arabidopsis thaliana*—have been identified as major $m^5C$ methyltransferases in eukaryotes [1,14,15]. In rice, OsNSUN2 mediates the $m^5C$ modification of photosynthesis-related transcripts and enhances their expression [16]. We recently demonstrated that TaNSUN2 functions as an $m^5C$ methyltransferase in wheat and is involved in susceptibility to Chinese wheat mosaic virus (CWMV) infection by directly methylating viral RNA. During infection, TaNSUN2 is recruited to viral replication complexes, where it deposits $m^5C$ marks on CWMV genomic RNAs to promote viral RNA stability and accumulation [17]. Similar strategies have been reported for other mammalian viruses, emphasizing that viral pathogens can hijack host RNA methyltransferases to facilitate replication [18,19]. Emerging evidence suggests that $m^5C$ modification can influence mRNA stability and translation [16,20], thereby shaping gene expression outcomes under stress conditions, including pathogen infection [17]. However, although the $m^5C$-mediated regulation of host transcripts has been reported in other systems, whether TaNSUN2 modulates host antiviral responses through the $m^5C$ modification of endogenous transcripts in wheat remains unclear.

CWMV is a soil-borne *furovirus* that poses a serious threat to wheat production [21] and causes wheat yellow mosaic disease, which leads to yield losses of 10–30% in affected fields and up to more than 70% in severe cases [22,23]. This disease has been widely reported in major winter wheat-producing regions of China, including Shandong, Jiangsu, Anhui, and Zhejiang provinces, and has shown a trend of spreading toward northern and western areas [24]. CWMV's bipartite positive-sense RNA genome consists of RNA1, which encodes replication-associated proteins and the movement protein (MP), and RNA2, which encodes the coat protein (CP) and a cysteine-rich protein (CRP) that functions as a suppressor of RNA silencing [21,25,26]. These viral proteins are essential for viral replication, movement, and host interaction, while viral accumulation is strongly influenced by environmental factors such as temperature [21,25,27]. Host defense against CWMV involves multiple layers of regulation, including reactive oxygen species (ROS) signaling [28,29]. ROS bursts represent a key component of plant basal immunity [30–32] during the battle between plants and viruses; specifically, they function as signaling molecules that activate downstream antiviral defenses and restrict viral infection [28]. Moreover, the expression of some endogenous genes is increased in plants in response to viral infections [33,34]. Previous studies have shown that the expression of the thiamine biosynthesis-related protein THI2 is upregulated in response to abiotic stress [35,36], and TaTHI2 has been identified as an endogenous CWMV resistance factor. During infection, TaTHI2 protein abundance is increased in the plasma membrane, which then interacts with the calcium-dependent protein kinase TaCPK5, suppressing catalase activity and promoting ROS accumulation, thus restricting viral spread [29]. Although TaTHI2 plays a central role in this antiviral pathway, its post-transcriptional regulation has not yet been characterized.

Given the emerging role of $m^5C$ in controlling mRNA fate and the importance of TaTHI2 in CWMV resistance, we hypothesized that *TaTHI2* mRNA is subjected to TaNSUN2-mediated $m^5C$ modifications during viral infection. In this study, we demonstrated that TaNSUN2 directly methylates *TaTHI2* mRNA, enhancing its stability, whereas the disruption of a key $m^5C$ site compromises ROS accumulation and promotes CWMV infection. Together, our results identify *TaTHI2* mRNA $m^5C$ modifications as a key post-transcriptional control point in ROS-mediated resistance to CWMV.

## 2. Materials and Methods

### *2.1. Plant Materials and Growth Conditions*

*Nicotiana benthamiana* plants were cultivated in a controlled growth chamber at 25 ± 2 °C with a 16 h light/8 h dark photoperiod and 65 ± 5% relative humidity. For viral infection assays, the wheat cultivar 'Fielder' was used, which is susceptible to CWMV. Wheat seedlings were initially grown in a greenhouse at 25 ± 2 °C. After reaching the four-leaf stage, the seedlings were rub-inoculated with CWMV and subsequently transferred to a growth chamber maintained at 15 ± 2 °C under a 16 h light/8 h dark cycle. Experimental analyses were conducted 14 dpi. Additionally, *TaNSUN2*-overexpressing (*TaNSUN2*-OE) and knockout (*TaNSUN2*-KO) wheat lines previously generated in our laboratory were used in this study.

### *2.2. Virus Inoculation and Agroinfiltration*

For transient expression in *N. benthamiana*, *Agrobacterium tumefaciens* strain GV3101 carrying pCB35S-R1 ($OD_{600}$ = 0.6–0.8) was mixed with an equal volume of GV3101 containing pCB35S-R2 or its mutants. The mixture was resuspended in infiltration buffer (100 mM MES; 10 mM $MgCl_2$; and 20 mM acetosyringone) and infiltrated into the abaxial sides of the leaves using needleless syringes. For wheat infection, CWMV RNA1 and RNA2 were in vitro transcribed using the Ambion Message Machine kit (Invitrogen; Carlsbad, CA, USA) after linearization with SpeI. Equal amounts (5 µg each) of the transcripts were diluted in 1× FES buffer and rub-inoculated onto the entire second leaves of the wheat seedlings. Each treatment included six seedlings and was repeated in three independent biological replicates. The inoculated plants were maintained at 15 °C, and viral disease signs were recorded at 14 dpi.

### *2.3. $m^5C$ RIP Assay*

Total RNA (200 µg) extracted from wheat plants was incubated in a final volume of 500 µL containing 1× IP buffer (50 mM Tris-HCl; 150 mM NaCl; 0.5% (*v*/*v*) Nonidet P-40), 200 U RNasin, and 10 µg anti-$m^5C$ antibody with gentle rotation for 2 h at 4 °C. Subsequently, 200 µL of protein A agarose beads pre-equilibrated in 1× IP buffer was added to the reaction, followed by an additional 2 h of rotation at 4 °C. The beads were collected via centrifugation and washed four times with 1× IP buffer. $m^5C$-enriched RNA was eluted via incubation with an elution competition buffer (50 mM Tris-HCl; 150 mM NaCl; 0.5% (*v*/*v*) Nonidet P-40; 200 U RNasin; and 6.7 mM free $m^5C$) for 1 h at room temperature with vigorous shaking. The eluted RNA was purified via phenol/chloroform extraction, followed by ethanol precipitation. Parallel immunoprecipitation reactions were performed using normal IgG as a negative control. The enriched RNA fragments were analyzed via RT-PCR and qRT-PCR using gene-specific primers, which are listed in Table S1.

### *2.4. Preparation of RNA Probe and MST Assay*

A Cy5-labeled RNA probe was commercially synthesized. For the binding assay, the labeled RNA probe was mixed with purified TaNSUN2-GST or GST alone (negative control) at predetermined ratios. The mixture was incubated in the dark for 2 min to allow for RNA–protein interactions. Subsequently, the samples were loaded into capillary tubes and analyzed using an MST instrument to examine the protein–RNA binding. Data were processed and analyzed using software provided by NanoTemper Technologies (Munich, Germany), and equilibrium dissociation constants for the interactions were calculated based on the obtained binding curves.

Cy5-labeled RNA probes corresponding to the indicated *TaTHI2* sequences were chemically synthesized. For the MST-binding assays, the labeled RNA probes were incubated

with the purified TaNSUN2-GST protein at various concentrations. Purified GST protein was used as a negative control. RNA–protein mixtures were prepared at predetermined molar ratios and incubated in the dark for 2 min to allow for complex formation. The samples were subsequently loaded into standard capillaries and analyzed using a microscale thermophoresis instrument (NanoTemper Technologies) according to the manufacturer's instructions. MST data were processed using the NanoTemper Analysis software, and the equilibrium dissociation constants ($K_d$) were calculated by fitting the binding curves.

### *2.5. Plasmid Construction*

The full-length coding sequence of *TaTHI2* was amplified from the cDNA derived from the wheat cultivar 'Fielder' and cloned into the pGWB454 vector. The TaNSUN2-GFP construct used in this study was generated and maintained in our laboratory.

### *2.6. RNA Stability Assay*

For the mRNA stability assays in *N. benthamiana*, recombinant expression constructs were introduced into leaves via Agrobacterium tumefaciens (GV3101)-mediated infiltration. After 36 h of expression, actinomycin D (Sigma, A4262; Shanghai Pureone Biotechnology, Shanghai, China) dissolved in $ddH_2O$ was infiltrated into the abaxial sides of leaves at a final concentration of 25 μg/mL using a needleless syringe. Each treatment included six infiltrated leaves per experiment, and the experiment was independently repeated three times to generate biological replicates. Leaf discs were collected immediately after actinomycin D infiltration and designated as the 0 h time point. Subsequent samples were harvested at 2 and 4 h post-treatment and immediately frozen in TRI reagent (Invitrogen) for RNA extraction. Total RNA was extracted using TRIzol reagent according to the manufacturer's instructions and treated with DNase I to remove genomic DNA contamination. First-strand cDNA was synthesized from 1 μg of total RNA using a reverse transcription kit. Quantitative PCR was performed using gene-specific primers to determine the relative transcript abundance at each time point. The transcript levels were normalized to the *N. benthamiana* reference gene *ubiquitin-conjugating enzyme* (*NbUBC*), and the RNA decay rates were calculated based on changes in the relative transcript levels over time.

### *2.7. Construction of Vector with Point Mutations*

The full-length $TaTHI2^{C830T}$ coding sequence was generated by amplifying two overlapping fragments of the *TaTHI2*-pGWB454 template using site-directed mutagenesis primers (Table S1). The two fragments were assembled into a full-length CDS using overlap extension PCR, and the resulting PCR products were cloned into the pGWB454 vector for the subsequent experiments.

### *2.8. Histochemical Staining for Hydrogen Peroxide ($H_2O_2$)*

To visualize the $H_2O_2$ accumulation, histochemical staining with DAB was performed according to a previously established protocol [32]. In this assay, DAB reacts with $H_2O_2$ in the presence of endogenous peroxidases to form a stable, dark-brown polymeric precipitate, thereby marking the sites of $H_2O_2$ localization. Briefly, leaf samples collected from agroinfiltrated *N. benthamiana* were submerged in DAB staining solution (Sigma-Aldrich; Merck KGaA; Darmstadt, Germany), incubated overnight in the dark, and then decolorized by boiling them in absolute ethanol until the chlorophyll was completely removed. For the quantitative analysis, the relative staining intensity was measured using the ImageJ 1.8.0 software (http://rsbweb.nih.gov/ij (accessed on 26 June 2025)), as described previously [37].

### *2.9. Western Blot Assay*

Total protein was extracted from homogenized *N. benthamiana* and wheat tissues using a lysis buffer containing 6% SDS, 100 mM Tris-HCl (pH 8.8), and 2% β-mercaptoethanol. Equal amounts of total protein (5 μg per lane) were mixed with SDS loading buffer, boiled at 95 °C for 10 min, and separated via SDS-PAGE on 12.5% polyacrylamide gels. Proteins were transferred onto nitrocellulose membranes using a wet transfer system. Following transfer, membranes were stained with Ponceau S to verify equal protein loading across lanes and were then blocked with 5% (*w*/*v*) skim milk in TBST for 60 min at room temperature and incubated with primary antibodies, including anti-CP (1:5000; HuaanBio; Hangzhou, China) and anti-RFP (1:2000; Chromo tek; Martinsried, Germany), followed by HRP-conjugated secondary antibodies (1:5000; TransGen Biotech; Beijing, China). Immunoreactive signals were detected using an enhanced chemiluminescence (ECL) substrate and visualized with an Amersham Imager 680 system, and band intensities were quantified using the ImageJ 1.8.0 software. The relative protein abundance was calculated by normalizing the band intensity to the control group, which was set to 1.0. Quantification was based on three independent biological replicates.

### *2.10. Statistical Analyses*

All statistical processing was performed using the GraphPad Prism 10.1.2 software (https://www.graphpad-prism.cn/?c=h&a=login (accessed on 14 September 2024)). Two-tailed Student's *t* test was applied for comparisons between two groups, while one-way analysis of variance (ANOVA) accompanied by Tukey's correction was adopted for comparisons among multiple groups. Statistical significance was defined as $p < 0.05$ and labeled as follows: * $p < 0.05$; ** $p < 0.01$; *** $p < 0.001$; n.s. represents no significant difference. The different lowercase letters represent significantly different means, and means followed by different lowercase letters are significantly different at the $p < 0.05$ level.

## 3. Results

### *3.1. m$^5$C Modifications of TaTHI2 mRNA in Wheat*

TaTHI2 has previously been identified as a key regulator of antiviral responses during CWMV infection [29]. Consistently, we observed a significant increase in *TaTHI2* transcripts upon viral infection (Figures 1a and S1). Given that post-transcriptional RNA modifications such as m$^5$C and m$^6$A are often associated with mRNA stability and expression [15], we next examined whether *TaTHI2* mRNA undergoes m$^5$C modification. Reanalysis of our previously generated RNA bisulfite sequencing data [17] revealed multiple candidate m$^5$C sites within *TaTHI2* transcripts. Notably, one site located at cytosine 830 (C830) was observed in wild-type plants but was notably absent in TaNSUN2-deficient lines (Figure 1b), suggesting that this modification is dependent on TaNSUN2, a previously characterized m$^5$C methyltransferase in wheat. Primers were designed to amplify a *TaTHI2* mRNA fragment encompassing the C830 region to further validate the presence of m$^5$C modification at this site. Total RNA extracted from 'Fielder' plants was subjected to m$^5$C RNA immunoprecipitation (m$^5$C-IP) using an anti-m$^5$C antibody, and RT-PCR analysis showed that the *TaTHI2* fragment was enriched in the immunoprecipitated fraction compared with the input (Figure 1c). Consistently, RIP-qPCR analysis further confirmed a significant enrichment of *TaTHI2* mRNA in the m$^5$C-IP samples (Figure 1d). Notably, a chemically synthesized RNA fragment lacking cytosine residues showed no detectable enrichment under the same conditions, whereas TaHSP70 (heat shock protein 70), a transcript previously reported to carry m$^5$C modification, was significantly enriched. Together, these results indicate that the enrichment of TaTHI2 reflects specific m$^5$C modification rather than nonspecific binding.

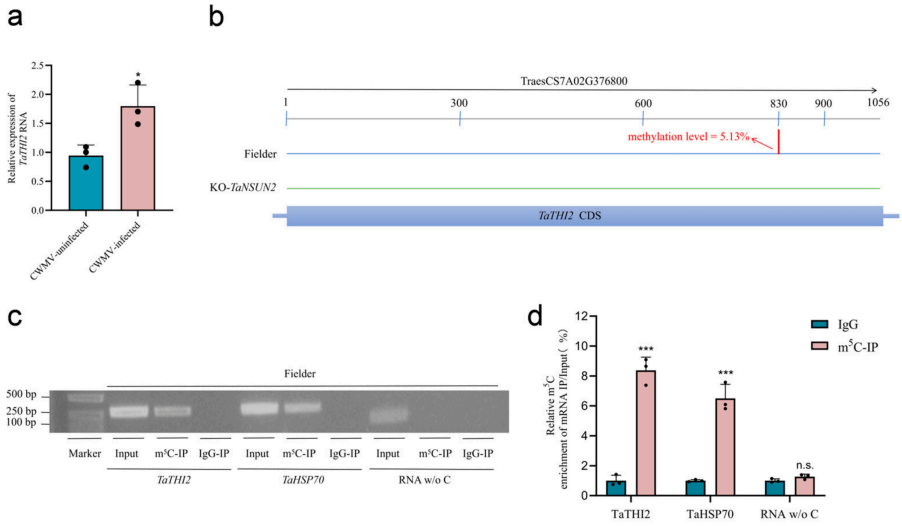



**Figure 1.** The transcriptional and m$^5$C modification status of *TaTHI2* in wheat. (**a**) The *TaTHI2* transcript abundance in CWMV-infected and mock-inoculated 'Fielder' plants at 14 dpi, determined via qRT-PCR. The data represent means ± SDs ($n$ = 3 biological replicates; two-sided $t$ test; * $p < 0.05$). (**b**) A visualization analysis diagram of the m$^5$C modification of IGV on *TaTHI2* mRNA of Fielder and *TaNSUN2*-KO. Each column represents the site where modification was detected, and the positions outlined in red are the C830 position (7A, 550052928). The range of methylation levels is 0–0.05. (**c**) Detection of m$^5$C-modified *TaTHI2* mRNA via m$^5$C RNA immunoprecipitation (m$^5$C-RIP) followed by RT-PCR. Total RNA extracted from 'Fielder' plants was immunoprecipitated using an anti-m$^5$C antibody or IgG as a negative control. *TaHSP70*, a known m$^5$C-modified transcript, was used as a positive control and showed clear enrichment in the m$^5$C-IP fraction. A chemically synthesized RNA fragment lacking cytosine residues (RNA w/o C) was used as a negative control and showed no detectable enrichment. (**d**) Quantification of mRNA enrichment in the m$^5$C-immunoprecipitated fraction via m$^5$C-RIP-qPCR. Data are the means ± SDs ($n$ = 3 biological replicates; two-sided $t$ test; *** $p < 0.001$, n.s. represents no significant difference).

### *3.2. Association Between TaNSUN2 and TaTHI2 mRNA and Its Effect on m$^5$C Modifications*

Total RNA was isolated from *TaNSUN2*-OE lines, *TaNSUN2*-KO lines, and the wild-type wheat cultivar 'Fielder' to determine whether TaNSUN2 regulates the m$^5$C modification of *TaTHI2* mRNA at the predicted C830 region. m$^5$C-modified RNAs were enriched via m$^5$C-IP using an anti-m$^5$C antibody, followed by RT-PCR and qRT-PCR analyses. RT-PCR analysis revealed a marked increase in the enrichment of the *TaTHI2* mRNA fragment, encompassing the C830 site, in the m$^5$C-immunoprecipitated samples from *TaNSUN2*-OE plants compared with that in 'Fielder' plants, whereas this fragment was undetectable in *TaNSUN2*-KO plants (Figure 2a). Consistent with these results, m$^5$C-RIP-qPCR analysis showed a significant increase in the relative m$^5$C level in the *TaTHI2* mRNA in *TaNSUN2*-OE lines and a pronounced decrease in *TaNSUN2*-KO lines relative to that in the wild-type (Figure 2b). Microscale thermophoresis (MST) assays were performed using the purified TaNSUN2-GST protein and a chemically synthesized *TaTHI2* RNA probe encompassing the C830 region to determine whether TaNSUN2 was directly associated with *TaTHI2* mRNA. In addition, a previously reported [17] CWMV RNA2 3′ UTR probe (designated as S2-P) was included as a positive control. Binding between TaNSUN2-GST and the *TaTHI2* RNA probe was detected via MST, with an apparent dissociation constant ($K_d$) of 2.79 nM, whereas no detectable interaction was observed between the *TaTHI2* RNA probe and GST under the same experimental conditions. The S2-P probe showed strong binding to TaNSUN2 under identical conditions, supporting the reliability of the assay (Figure 2c). Given the association between the TaNSUN2 and *TaTHI2* mRNA levels, we examined the effect of TaNSUN2 on the *TaTHI2* mRNA stability. Following transcriptional inhibition,

*TaTHI2* transcripts exhibited a slower decay rate in the presence of transiently expressed TaNSUN2-GFP than that in the control sample (Figure 2d).

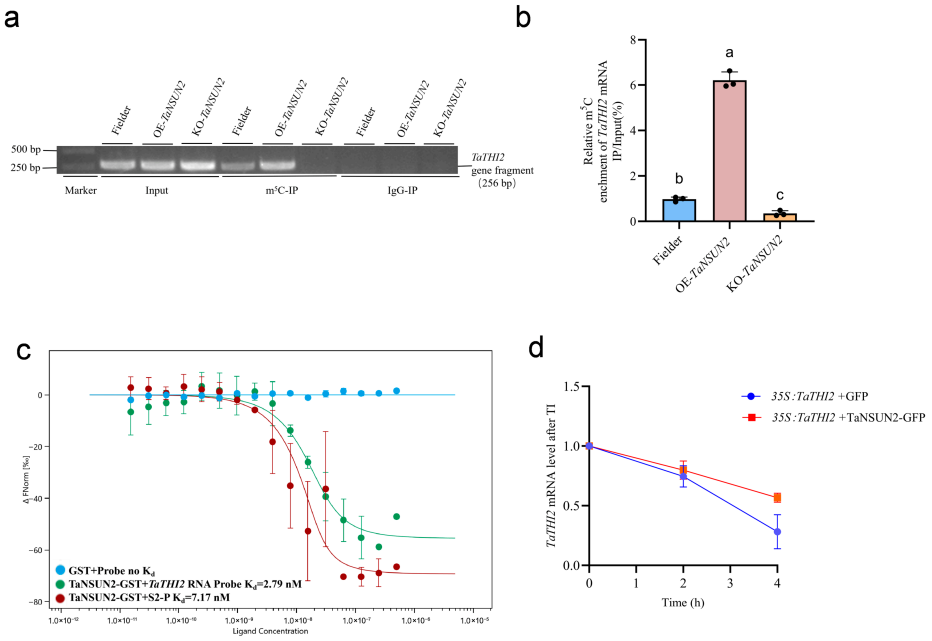



**Figure 2.** TaNSUN2-mediated m$^5$C modification of *TaTHI2* mRNA. (**a**) Detection of m$^5$C modification on *TaTHI2* mRNA via m$^5$C RNA immunoprecipitation (m$^5$C-RIP) followed by RT-PCR. Total RNA from 'Fielder', *TaNSUN2*-OE, and *TaNSUN2*-KO wheat plants was subjected to m$^5$C-RIP using anti-m$^5$C antibody. Input and IgG-immunoprecipitated samples were included as controls. (**b**) Quantification of *TaTHI2* mRNA m$^5$C modifications via m$^5$C-RIP-qPCR. Enrichment levels were normalized to input RNA. Values represent means ± SDs ($n$ = 3 biological replicates; one-way ANOVA with Tukey's multiple comparisons test; different lowercase letters indicate significant differences; $p < 0.05$). (**c**) Direct association between TaNSUN2 and *TaTHI2* mRNA analyzed via microscale thermophoresis (MST). Purified TaNSUN2-GST protein was incubated with chemically synthesized *TaTHI2* RNA probe encompassing C830 region. GST protein incubated with same RNA probe served as negative control, and TaNSUN2-GST protein incubated with S2-P probe was used as positive control. Data are presented as means ± SDs ($n$ = 3). (**d**) Analysis of *TaTHI2* mRNA stability following transcriptional inhibition (TI) in presence or absence of TaNSUN2. Data represent means ± SDs ($n$ = 3 biological replicates).

### *3.3. Cytosine 830 Contributes to the m$^5$C Modification of TaTHI2 mRNA*

The potential effects of different C830 substitutions were first evaluated in silico to assess whether C830 represents a major m$^5$C modification site on *TaTHI2* mRNA. RNAfold was used to predict changes in the RNA secondary structure resulting from the substitution of C830 for A, U, or G. Among the tested substitutions, the replacement of C830 with U least affected the predicted secondary structure of *TaTHI2* mRNA (Figure 3a) and was therefore selected for subsequent analyses. Meanwhile, structural prediction indicated that the C830T mutation exerted no obvious effect on the three-dimensional conformation of the resulting protein (Figure 3b). Furthermore, we constructed m$^5$C-inactivation mutant forms of *TaTHI2*$^{C830T}$ and *TaTHI2*, and these were then transiently introduced into wheat protoplasts (Figure 3c). m$^5$C-IP was performed using wheat protoplasts transiently expressing TaTHI2-RFP or TaTHI2$^{C830T}$-RFP. RT-PCR analysis showed a reduction in the enrichment of the m$^5$C-immunoprecipitated *TaTHI2*$^{C830T}$ mRNA fragment compared with that with the wild-type *TaTHI2* transcript (Figure 3d), and m$^5$C-RIP-qPCR analysis consistently revealed a significant decrease in the m$^5$C modification of *TaTHI2* mRNA following the substitution of C830 with T (Figure 3e). Next, we examined whether the C830-to-T substitution affected

the interaction between TaNSUN2 and *TaTHI2* mRNA. MST assays were performed using purified TaNSUN2-GST together with chemically synthesized RNA probes corresponding to wild-type *TaTHI2* or the C830T variant. The C830T substitution markedly reduced the binding affinity of TaNSUN2 for *TaTHI2* mRNA, as reflected by the substantially increased dissociation constant compared to that of the wild-type probe (Figure 3f). *TaTHI2*$^{C830T}$ mRNA decayed more rapidly than the wild-type transcript following transcriptional inhibition, indicating that the substitution at C830 was associated with a reduction in *TaTHI2* mRNA stability (Figure 3g).

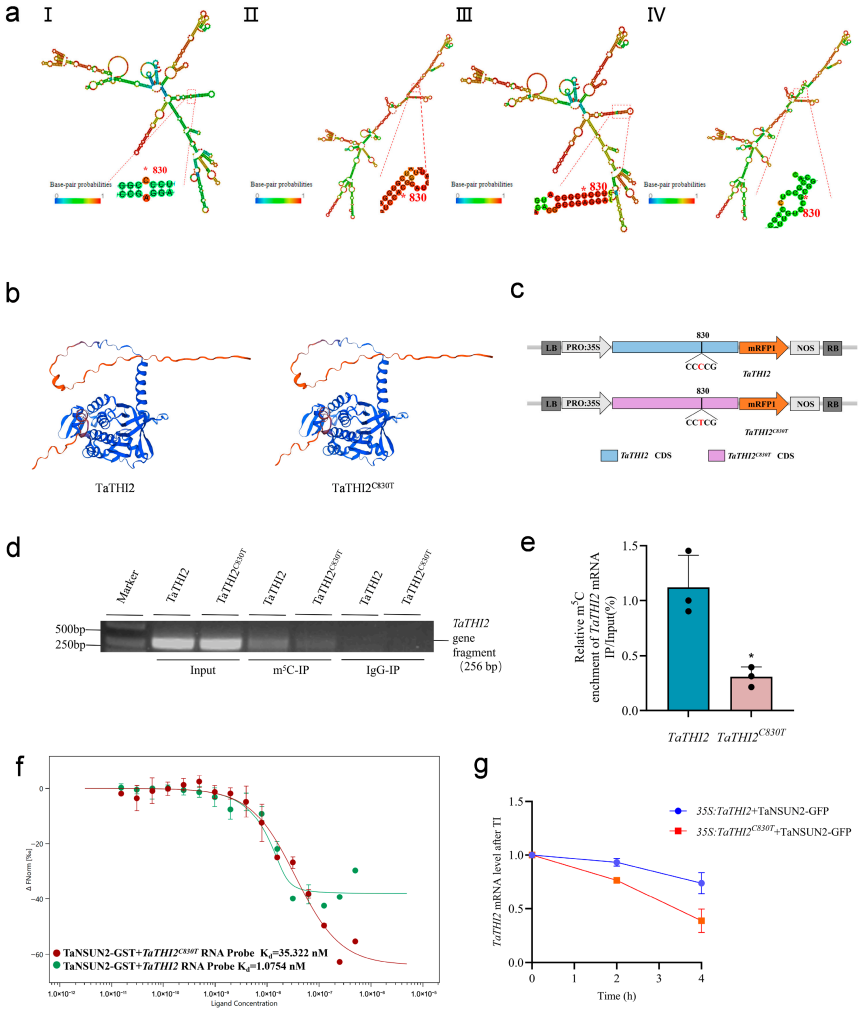



**Figure 3.** C830 is a critical m$^5$C modification site in *TaTHI2* mRNA. (**a**) The predicted secondary structure of *TaTHI2* mRNA after the substitution of cytosine 830 (C830) with adenine (A), uracil (U), and guanine (G). Panel I shows the predicted secondary structure of wild-type *TaTHI2* mRNA, whereas panels II–IV show the predicted structures following the substitution of C830 with A, U, and G, respectively. The C830 position is indicated by red asterisks. (**b**) A three-dimensional structure prediction map of the wild-type TaTHI2 and mutant TaTHI2 protein sequences using the SWISS MODEL tool. Different colors correspond to different confidence levels. Red represents low confidence, whereas blue indicates high confidence. (**c**) A schematic representation of the *TaTHI2* mutation used in the subsequent validation assays. The coding regions of the wild-type *TaTHI2* and mutant *TaTHI2*$^{C830T}$ were cloned into the pGWB454 expression vector driven by the CaMV 35S promoter. (**d**) m$^5$C RNA immunoprecipitation (RIP) analysis of *TaTHI2* and *TaTHI2*$^{C830T}$ mRNA. RIP assays were performed using an anti-m$^5$C antibody or IgG as a negative control on total RNA isolated from *Nicotiana benthamiana* leaves transiently expressing *TaTHI2* or *TaTHI2*$^{C830T}$. Enriched *TaTHI2* mRNA fragments were detected via RT-PCR and agarose gel electrophoresis. (**e**) Quantification of the m$^5$C modification levels of *TaTHI2* and *TaTHI2*$^{C830T}$ mRNA via m$^5$C-RIP-qPCR. The enrichment of *TaTHI2* mRNA fragments, shown in panel (**c**),

was calculated. Values represent means ± SDs ($n$ = 3 biological replicates; two-sided $t$ test; * $p < 0.05$). (**f**) The interaction between TaNSUN2 and *TaTHI2* mRNA was analyzed via microscale thermophoresis (MST). The purified TaNSUN2-GST protein was incubated with chemically synthesized RNA probes corresponding to wild-type *TaTHI2* or the C830T variant. Each binding assay was performed three times independently, and data are presented as means ± SDs. (**g**) Stability analysis of *TaTHI2* and *TaTHI2*$^{C830T}$ mRNA in the presence of TaNSUN2 following transcriptional inhibition (TI). Data are shown as means ± SDs ($n$ = 3 biological replicates).

### *3.4. C830-to-T Mutation in TaTHI2 mRNA Reduces ROS Accumulation and Facilitates CWMV Infection*

We compared the effects of wild-type *TaTHI2* mRNA and mutant *TaTHI2*$^{C830T}$ mRNA to evaluate the effect of the *TaTHI2*$^{C830T}$ mutation on CWMV accumulation. As *TaTHI2* is known to trigger an ROS burst signaling cascade that confers CWMV infection resistance, ROS accumulation serves as an additional indicator for assessing viral infection [29]. *N. benthamiana* leaves were co-infiltrated with CWMV and RFP, TaTHI2-RFP, or TaTHI2$^{C830T}$-RFP to assess the effect of the C830-to-T mutation in *TaTHI2* on the ROS production and CWMV accumulation. The ROS accumulation was analyzed via 3,3′-diaminobenzidine (DAB) staining and quantified using ImageJ. The ROS levels were markedly increased in leaves expressing either TaTHI2-RFP or TaTHI2$^{C830T}$-RFP compared with those of the CWMV+RFP control. However, the ROS accumulation was significantly lower in TaTHI2$^{C830T}$-RFP-expressing leaves than in those expressing TaTHI2-RFP (Figure 4a,b). The CWMV accumulation was further assessed via qRT-PCR and Western blotting. Consistent with the ROS results, both the CWMV RNA and CP levels were significantly reduced in leaves expressing TaTHI2-RFP or TaTHI2$^{C830T}$-RFP compared with those in the control. Notably, viral accumulation was higher in TaTHI2$^{C830T}$-RFP-expressing leaves than in those expressing TaTHI2-RFP (Figure 4c,d).

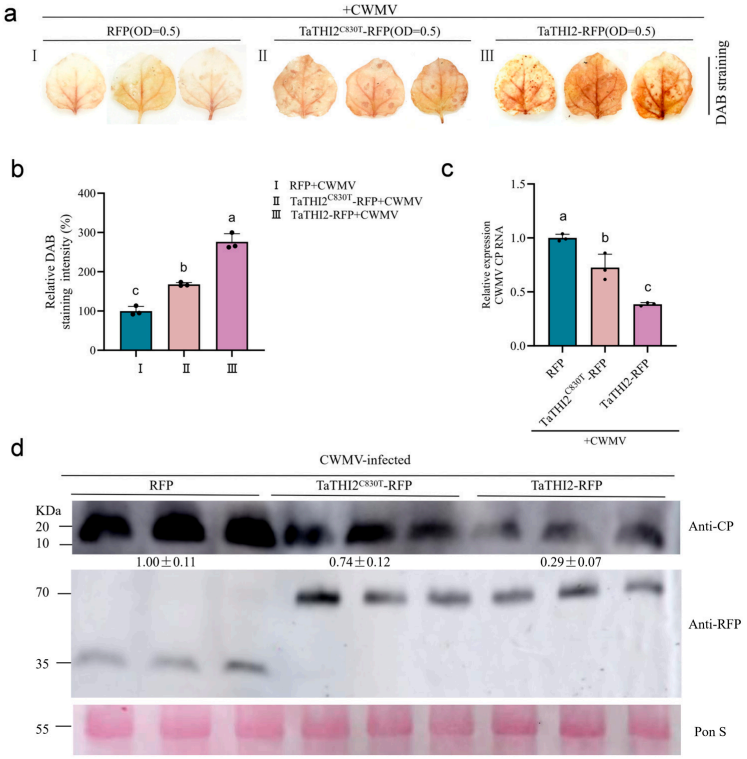



**Figure 4.** The *TaTHI2*$^{C830T}$ mutant of *TaTHI2* mRNA facilitates Chinese wheat mosaic virus (CWMV) infection by reducing reactive oxygen species (ROS) accumulation. (**a**) *Nicotiana benthamiana* leaves

were co-infiltrated with CWMV and TaTHI2-RFP, TaTHI2$^{C830T}$-RFP, or RFP alone, with CWMV + RFP serving as the control. Leaves were stained with 3,3′-diaminobenzidine (DAB) to detect ROS production. (**b**) Measurement of the relative DAB staining intensity as shown in (**a**). Values were obtained by measuring three representative images chosen from three biological replicates, and the data presented are the means ± SDs from three samples; different lowercase letters indicate significant differences ($p < 0.05$). (**c**) Accumulation of CWMV RNA in the inoculated leaves from (**a**), as analyzed via qRT-PCR. Data represent means ± SDs. Different letters show statistically significant differences ($p < 0.05$, Tukey's test). (**d**) CWMV accumulation in these *N. benthamiana* leaves was detected via Western blotting using an anti-CWMV CP and anti-RFP antibody.

## 4. Discussion

Post-transcriptional RNA modifications are important regulators of plant stress adaptation and immunity [9–11]. In the CWMV–wheat pathosystem, TaTHI2 functions as an endogenous resistance factor that restricts viral infection by modulating TaCPK5–catalase signaling and ROS accumulation [29]. Consistent with these findings, *TaTHI2* transcripts responded to CWMV infection, with altered expression dynamics observed between infected and mock-treated plants, and they showed consistent expression across infection stages and tissues associated with viral accumulation (Figures 1a and S1). Previous RNA-BisSeq analysis identified m$^5$C modification sites within TaTHI2 transcripts, among which the C830 site showed both a high sequencing depth and methylation level, suggesting that it represents a reliable and potentially functional modification site [17]. Building on this observation, we further validated this site and investigated its functional relevance. Together with m$^5$C site prediction and m$^5$C-RIP validation, these results established *TaTHI2* as an infection-associated host factor and prompted an investigation of its post-transcriptional regulation (Figure 1c,d). Among RNA modifications, m$^6$A has been extensively linked to developmental regulation, stress adaptation, and viral infection [38]; however, functional evidence of its involvement in plant immunity remains limited. NSUN family methyltransferases regulate mRNA fates in plants, as exemplified by the OsNSUN2-mediated m$^5$C modification of photosynthesis-related transcripts in rice [16]. In wheat, TaNSUN2 acts as an mRNA m$^5$C methyltransferase and is exploited by CWMV to enhance viral infection via viral RNA methylation [17]. Extending these findings, we showed that *TaTHI2* mRNA undergoes TaNSUN2-dependent m$^5$C modification in plants, as revealed via RT-PCR-based detection and quantitative m$^5$C-RIP-qPCR following enrichment with an anti-m$^5$C antibody (Figure 2a,b). TaNSUN2 was found to directly associate with *TaTHI2* RNA (Figure 2c) and to contribute to the m$^5$C modification of *TaTHI2* transcripts, enhancing mRNA stability (Figure 2d) and, thus, establishing m$^5$C as a determinant of *TaTHI2* transcript stability during infection.

RNA methylation frequently occurs in a site-specific manner, with individual modified nucleotides exerting pronounced effects on transcript fates [4,14,15]. Given the prominent cytosine identified in *TaTHI2* mRNA (Figure 1d), we next examined its functional relevance. Guided by the RNA secondary structure prediction (Figure 3a), a C-to-T substitution was introduced to minimally perturb transcript folding while disrupting the predicted m$^5$C site (Figure 3c). This single-site mutation markedly reduced m$^5$C enrichment (Figure 3d,e), weakened TaNSUN2–RNA binding (Figure 3f), and accelerated transcript decay (Figure 3g). Although this substitution introduces a conservative amino acid change, structural modeling using SWISS-MODEL revealed no obvious global differences between the wild-type and mutant TaTHI2 proteins (Figure 3b), suggesting limited impact on the overall protein folding. Nevertheless, a contribution from altered protein properties cannot be completely excluded. Given that the m$^5$C modification has been reported to primarily regulate RNA

stability and RNA–protein interactions [4,14,15], together with the coordinated loss of methylation, RNA binding, and transcript stability observed in this study, we propose that these effects are mainly attributable to disruption of the $m^5C$ regulatory axis. Consistent with the established role of TaTHI2 in ROS-mediated resistance [29], the loss of the *TaTHI2* $m^5C$ modification significantly reduced the ROS accumulation, as shown by the DAB staining and quantitative analysis (Figure 4a,b), and concomitantly increased the CWMV RNA and CP levels (Figure 4c,d). These results directly link $m^5C$-dependent transcript stabilization to ROS-mediated antiviral defense.

Plant viruses commonly hijack the host RNA modification machinery to favor replication [38]. In wheat, TaNSUN2 is recruited to the CWMV replication complexes to deposit $m^5C$ marks on viral RNAs, enhancing the viral RNA stability and accumulation [17]. Our findings revealed that TaNSUN2 simultaneously targets the host resistance transcript *TaTHI2*, indicating a dual role in the CWMV pathosystem. Accordingly, we put forward a hypothesis explaining the dynamic alterations in substrate allocation within wheat plants upon CWMV infection. The early TaNSUN2-mediated stabilization of *TaTHI2* may contribute to the initial host defense. As the infection progresses, viral recruitment increasingly biases TaNSUN2 activity toward viral RNA, ultimately favoring infection. The partial retention of host-directed methylation likely generates a competitive balance between viral exploitation and host defense maintenance. While our results establish a functional link between TaNSUN2-mediated $m^5C$ modification and TaTHI2-dependent antiviral defense, the mechanisms underlying the substrate selection and downstream interpretation of $m^5C$ marks remain to be further explored.

Collectively, our findings support a model in which TaNSUN2 modulates host antiviral immunity by mediating the $m^5C$ modification of the *TaTHI2* transcript and elevating its mRNA stability (Figure 5). This modification stabilizes *TaTHI2* transcripts, sustains TaTHI2 accumulation, and promotes ROS-mediated defense against CWMV. Disruption of the $m^5C$-dependent regulatory axis compromises *TaTHI2* stability, attenuates ROS production, and facilitates viral infection. These findings suggest that *TaTHI2* mRNA $m^5C$ modification is a key post-transcriptional control point in CWMV resistance, highlight TaNSUN2-dependent RNA methylation as an integral component of host antiviral defense, and further implicate the $m^5C$-mediated regulation of host transcripts in plant antiviral immunity.

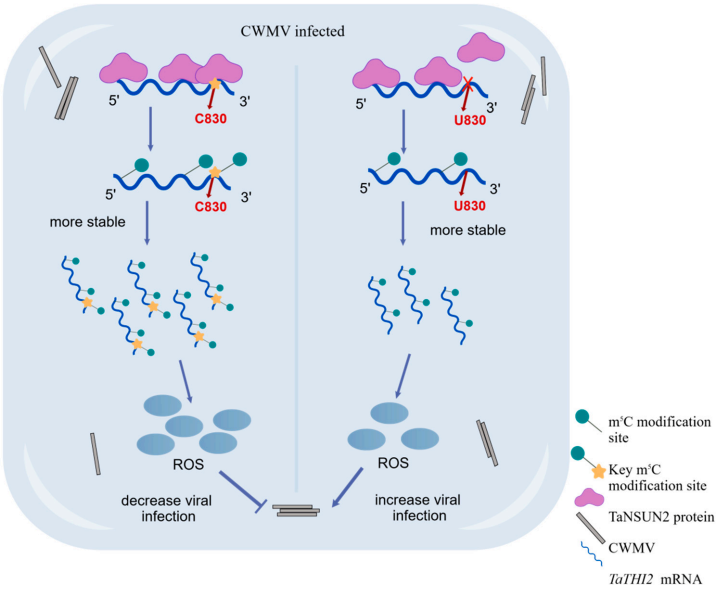



**Figure 5.** Working model of TaNSUN2-mediated $m^5C$ regulation of *TaTHI2* during Chinese wheat mosaic virus (CWMV) infection. During CWMV infection, TaNSUN2 binds TaTHI2 mRNA and is associated

with $m^5C$ modification at cytosine 830 (C830). This modification enhances *TaTHI2* mRNA stability, sustains TaTHI2 accumulation, and promotes reactive oxygen species (ROS) production, thereby restricting CWMV infection. The disruption of $m^5C$ modifications at C830 leads to reduced *TaTHI2* mRNA stability, decreased ROS accumulation, and enhanced viral infection. In addition, the yellow stars in the figure mark the C830 site with the potential for $m^5C$ modification, whereas the crosses represent the U830 site that is not subject to $m^5C$ modification.

**Supplementary Materials:** The following supporting information can be downloaded at https://www.mdpi.com/article/10.3390/agronomy16090921/s1. Figure S1: Phenotypic responses and viral coat protein accumulation in wheat cultivar 'Fielder' following CWMV infection; Table S1: Primers used in this study.

**Author Contributions:** Conceptualization, L.C., M.Z., J.Y. and Y.J.; methodology, L.C., M.Z., Y.W., L.F. and Y.L.; validation, L.C., M.Z., Y.W., L.F. and Y.L.; formal analysis, L.C., M.Z., Y.W. and L.F.; investigation, L.C., M.Z., Y.W., L.F., Y.L. and J.L.; resources, L.C., M.Z., Y.W. and J.L.; data curation, L.C., M.Z., Y.W., L.F. and Y.L.; writing—original draft, L.C., M.Z. and Y.J.; writing—review and editing, L.C., M.Z., Y.W., L.F., Y.L., J.L., J.Y. and Y.J.; visualization, L.C., M.Z., Y.W. and L.F.; supervision, J.Y.; project administration, J.Y. and Y.J.; funding acquisition, J.Y. and Y.J. All authors have read and agreed to the published version of the manuscript.

**Funding:** This research was funded by the Zhejiang Provincial Natural Science Foundation of China (grant no. LMS25C140004), the National Key Research and Development Program of China (grant no. 2024YFD1400402), the National Natural Science Foundation of China (grant no. 32372488), the China Postdoctoral Science Foundation (grant no. 2025M783810), and the Ningbo Natural Science Foundation (grant no. 2025J192).

**Data Availability Statement:** The original contributions presented in this study are included in the article/Supplementary Materials. Further inquiries can be directed to the corresponding authors.

**Conflicts of Interest:** The authors declare no conflicts of interest.

## References

1. Burgess, A.L.; David, R.; Searle, I.R. Conservation of tRNA and rRNA 5-methylcytosine in the kingdom Plantae. *BMC Plant Biol.* **2015**, *15*, 199. [CrossRef]
2. Shu, X.; Li, W.P. Chemical decoding strategies for detecting RNA modifications, dynamics and structures. *Chem. Commun.* **2025**, *61*, 12069–12084. [CrossRef]
3. Haruka, M.; Corina, N. Potential Roles of m6A and FTO in Synaptic Connectivity and Major Depressive Disorder. *Int. J. Mol. Sci.* **2023**, *24*, 6220. [CrossRef]
4. Wiener, D.; Schwartz, S. The epitranscriptome beyond m(6)A. *Nat. Rev. Genet.* **2021**, *22*, 119–131. [CrossRef] [PubMed]
5. Guo, S.T.; Li, Z.; Li, X.B.; Liang, Z.; Zhao, D.D.; Sun, N.; Liu, J.Q.; Wang, X.N.; Mei, S.; Qiao, X.Y.; et al. 2′-O-methylation and N6-methyladenosine enhance the oral delivery of small RNAs in mice. *Mol. Ther.-Nucleic Acids* **2025**, *36*, 102574. [CrossRef] [PubMed]
6. Zheng, Y.Y.; Wu, Y.; Begley, T.J.; Sheng, J. Sulfur modification in natural RNA and therapeutic oligonucleotides. *RSC Chem. Biol.* **2021**, *2*, 990–1003. [CrossRef]
7. Roundtree, I.A.; Evans, M.E.; Pan, T.; He, C. Dynamic RNA Modifications in Gene Expression Regulation. *Cell* **2017**, *169*, 1187–1200. [CrossRef]
8. Li, Z.L.; Xie, Y.; Wang, Y.F.; Wang, J.; Zhou, X.; Zhang, X.L. NSUN2-mediated HCV RNA m5C Methylation Facilitates Viral RNA Stability and Replication. *Genom. Proteom. Bioinform.* **2025**, *23*, qzaf008. [CrossRef]
9. Cui, X.; Liang, Z.; Shen, L.S.; Zhang, Q.; Bao, S.J.; Geng, Y.K.; Zhang, B.; Leo, V.; Vardy, L.A.; Lu, T.G.; et al. 5-Methylcytosine RNA Methylation in Arabidopsis Thaliana. *Mol. Plant* **2017**, *10*, 1387–1399. [CrossRef]
10. Wu, J.; Peled-Zehavi, H.; Galili, G. The m(6) A reader ECT2 post-transcriptionally regulates proteasome activity in Arabidopsis. *New Phytol.* **2020**, *228*, 151–162. [CrossRef] [PubMed]
11. Hu, J.; Cai, J.; Park, S.J.; Lee, K.; Li, Y.; Chen, Y.; Yun, J.Y.; Xu, T.; Kang, H. N(6)-Methyladenosine mRNA methylation is important for salt stress tolerance in Arabidopsis. *Plant J.* **2021**, *106*, 1759–1775. [CrossRef]

12. Chen, T.; Greene, G.H.; Motley, J.; Mwimba, M.; Luo, G.Z.; Xu, G.Y.; Karapetyan, S.; Xiang, Y.Z.; Liu, C.; He, C.; et al. m(6)A modification plays an integral role in mRNA stability and translation during pattern-triggered immunity. *Proc. Natl. Acad. Sci. USA* **2024**, *121*, e2411100121. [CrossRef] [PubMed]
13. Yang, X.; Yang, Y.; Sun, B.F.; Chen, Y.S.; Xu, J.W.; Lai, W.Y.; Li, A.; Wang, X.; Bhattarai, D.P.; Xiao, W.; et al. 5-methylcytosine promotes mRNA export—NSUN2 as the methyltransferase and ALYREF as an m(5)C reader. *Cell Res.* **2017**, *27*, 606–625. [CrossRef]
14. Squires, J.E.; Patel, H.R.; Nousch, M.; Sibbritt, T.; Humphreys, D.T.; Parker, B.J.; Suter, C.M.; Preiss, T. Widespread occurrence of 5-methylcytosine in human coding and non-coding RNA. *Nucleic Acids Res.* **2012**, *40*, 5023–5033. [CrossRef] [PubMed]
15. David, R.; Burgess, A.; Parker, B.; Li, J.; Pulsford, K.; Sibbritt, T.; Preiss, T.; Searle, I.R. Transcriptome-Wide Mapping of RNA 5-Methylcytosine in Arabidopsis mRNAs and Noncoding RNAs. *Plant Cell* **2017**, *29*, 445–460. [CrossRef] [PubMed]
16. Tang, Y.; Gao, C.C.; Gao, Y.; Yang, Y.; Shi, B.; Yu, J.L.; Lyu, C.; Sun, B.F.; Wang, H.L.; Xu, Y.; et al. OsNSUN2-Mediated 5-Methylcytosine mRNA Modification Enhances Rice Adaptation to High Temperature. *Dev. Cell* **2020**, *53*, 272–286. [CrossRef]
17. Jiang, Y.Y.; Liu, P.; Zhang, M.C.; Yong, B.; Yin, J.L.; Chen, L.W.; Shi, C.N.; Li, P.; Guo, Y.F.; Hu, H.C.; et al. Enhancing plant antiviral responses and productivity through the elimination of m(5)C methyltransferase. *Sci. Adv.* **2026**, *12*, eaea4046. [CrossRef]
18. Feng, J.P.; Xu, T.M.; He, M.; Li, J.L.; Yao, P.P.; Ma, C.B.; Yang, S.M.; Xu, Z.C.; Yan, K.; Chen, X.Y.; et al. NSUN2-mediated m5C modification of HBV RNA positively regulates HBV replication. *PLoS Pathog.* **2023**, *19*, e1011808. [CrossRef]
19. Ding, S.; Liu, H.B.; Liu, L.J.; Ma, L.; Chen, Z.; Zhu, M.; Liu, L.S.; Zhang, X.Y.; Hao, H.J.; Zuo, L.; et al. Epigenetic addition of m(5)C to HBV transcripts promotes viral replication and evasion of innate antiviral responses. *Cell Death Dis.* **2024**, *15*, 39. [CrossRef]
20. Zuo, S.; Li, L.; Wen, X.; Gu, X.; Zhuang, A.; Li, R.; Ye, F.; Ge, S.; Fan, X.; Fan, J.; et al. NSUN2-mediated m(5) C RNA methylation dictates retinoblastoma progression through promoting PFAS mRNA stability and expression. *Clin. Transl. Med.* **2023**, *13*, e1273. [CrossRef]
21. Diao, A.; Chen, J.P.; Ye, R.; Zheng, T.; Yu, S.Q.; Antoniw, J.F.; Adams, M.J. Complete sequence and genome properties of Chinese wheat mosaic virus, a new furovirus from China. *J. Gen. Virol.* **1999**, *80*, 1141–1145. [CrossRef]
22. Chen, J.P. Occurrence of fungally transmitted wheat mosaic viruses in China. *Ann. Appl. Biol.* **2010**, *123*, 55–61.
23. Ye, R.; Zheng, T.; Chen, J.; Diao, A.; Adams, M.J.; Yu, S.; Antoniw, J.F. Characterization and partial sequence of a new furovirus of wheat in China. *Plant Pathol.* **1999**, *48*, 379–387. [CrossRef]
24. Guo, L.M.; Jing, H.; Jing, L.; Chen, J.P.; Zhang, H.M. Chinese wheat mosaic virus: A long-term threat to wheat in China. *J. Integr. Agric.* **2019**, *18*, 821–829. [CrossRef]
25. Sun, L.Y.; Andika, I.B.; Shen, J.F.; Yang, D.; Ratti, C.; Chen, J.P. The CUG-initiated larger form coat protein of Chinese wheat mosaic virus binds to the cysteine-rich RNA silencing suppressor. *Virus Res.* **2013**, *177*, 66–74. [CrossRef] [PubMed]
26. Yang, J.; Zhang, F.; Xie, L.; Song, X.J.; Li, J.; Chen, J.P.; Zhang, H.M. Functional identification of two minor capsid proteins from Chinese wheat mosaic virus using its infectious full-length cDNA clones. *J. Gen. Virol.* **2016**, *97*, 2441–2450. [CrossRef] [PubMed]
27. Andika, I.B.; Sun, L.Y.; Xiang, R.; Li, J.M.; Chen, J.P. Root-specific role for Nicotiana benthamiana RDR6 in the inhibition of Chinese wheat mosaic virus accumulation at higher temperatures. *Mol. Plant-Microbe Interact.* **2013**, *26*, 1165–1175. [CrossRef]
28. Li, P.; Zhao, L.L.; Qi, F.; Htwe, N.M.P.S.; Li, Q.Y.; Zhang, D.W.; Lin, F.C.; Shang-Guan, K.K.; Liang, Y. The receptor-like cytoplasmic kinase RIPK regulates broad-spectrum ROS signaling in multiple layers of plant immune system. *Mol. Plant* **2021**, *14*, 1652–1667. [CrossRef]
29. Yang, J.; Chen, L.; Zhang, J.; Liu, P.; Chen, M.; Chen, Z.H.; Zhong, K.L.; Liu, J.Q.; Chen, J.P.; Yang, J. TaTHI2 interacts with Ca(2+)-dependent protein kinase TaCPK5 to suppress virus infection by regulating ROS accumulation. *Plant Biotechnol. J.* **2024**, *22*, 1335–1351. [CrossRef]
30. Waszczak, C.; Carmody, M.; Kangasjarvi, J. Reactive Oxygen Species in Plant Signaling. *Annu. Rev. Plant Biol.* **2018**, *69*, 209–236. [CrossRef] [PubMed]
31. Mittler, R.; Vanderauwera, S.; Suzuki, N.; Miller, G.; Tognetti, V.B.; Vandepoele, K.; Gollery, M.; Shulaev, V.; Van Breusegem, F. ROS signaling: The new wave? *Trends Plant Sci.* **2011**, *16*, 300–309. [CrossRef] [PubMed]
32. Wu, J.G.; Yang, R.X.; Yang, Z.R.; Yao, S.Z.; Zhao, S.S.; Wang, Y.; Li, P.C.; Song, X.W.; Jin, L.; Zhou, T.; et al. ROS accumulation and antiviral defence control by microRNA528 in rice. *Nat. Plants* **2017**, *3*, 16203. [CrossRef]
33. Tu, C.W.; Huang, Y.W.; Lee, C.W.; Kuo, S.Y.; Lin, N.S.; Hsu, Y.H.; Hu, C.C. Argonaute 5-mediated antiviral defense and viral counter-defense in *Nicotiana benthamiana*. *Virus Res.* **2023**, *334*, 179–199. [CrossRef]
34. Zhong, K.L.; Xu, G.C.; Shi, J.J.; Liu, P.; Tu, A.Z.; Wu, M.L.; Liu, J.Q.; Chen, J.P.; Yang, J. NbPIRIN promotes the protease activity of papain-like cysteine protease NbRD21 to inhibit Chinese wheat mosaic virus infection. *PLoS Pathog.* **2025**, *21*, e1013037. [CrossRef]
35. Idris, Z.H.C.; Abidin, A.A.Z.; Subki, A.; Yusof, Z.N.B. The Effect of Oxidative Stress Towards The Expression of Thiamine Biosynthesis Genes (THIC and THI1/THI4) in Oil Palm (*Elaeis guineensis*). *Trop. Life Sci. Res.* **2018**, *29*, 71–85. [CrossRef] [PubMed]
36. Rapala-Kozik, M.; Wolak, N.; Kujda, M.; Banas, A.K. The upregulation of thiamine (vitamin B1) biosynthesis in Arabidopsis thaliana seedlings under salt and osmotic stress conditions is mediated by abscisic acid at the early stages of this stress response. *BMC Plant Biol.* **2012**, *12*, 2–16. [CrossRef] [PubMed]

37. Sun, Y.D.; Folimonova, S.Y. The p33 protein of Citrus tristeza virus affects viral pathogenicity by modulating a host immune response. *New Phytol.* **2019**, *221*, 2039–2053. [CrossRef]
38. Guo, J.; Zhang, T.Y.; Xie, H.X.; Hu, H.C.; Shi, C.N.; Zhao, Y.J.; Yin, J.L.; Xu, G.C.; Wu, Z.C.; Wang, P.K.; et al. An m(6)A methyltransferase confers host resistance by degrading viral proteins through ubiquitination. *Nat. Commun.* **2025**, *16*, 4821. [CrossRef]

**Disclaimer/Publisher's Note:** The statements, opinions and data contained in all publications are solely those of the individual author(s) and contributor(s) and not of MDPI and/or the editor(s). MDPI and/or the editor(s) disclaim responsibility for any injury to people or property resulting from any ideas, methods, instructions or products referred to in the content.